This is to certify that the

thesis entitled

OPTIMIZATION OF TUBE HYDROFORMING PROCESS

presented by

Naeem Zafar

has been accepted towards fulfillment of the requirements for

MS degree in Mechanical Engineering

Ronald C. Averill
Major professor

Date 8/13/02

OPTIMIZATION
OF TUBE HYDROFORMING
PROCESS

By

Naeem Zafar

A THESIS

Submitted to
Michigan State University
in partial fulfillment of the requirements
for the degree of

MASTER OF SCIENCE

Department of Mechanical Engineering

2002

ABSTRACT

OPTIMIZATION OF TUBE HYDROFORMING PROCESS

By

Naeem Zafar

This thesis presents an approach to optimize the tube hydroforming process using a Genetic Algorithm (GA). A GA in combination with a structural finite element code is used to optimize the internal hydraulic pressure and feed rate while satisfying the forming limit diagram (FLD). Aside from the target of cost reduction, the industrial enterprises are aiming for optimization of their products regarding weight as well as stability and rigidity. This requires reevaluation of conventional design solutions, manufacturing techniques and material selections in the search for alternative solutions. Such an alternative with interesting technical and economical potential is hydroforming, a method for manufacturing a wide range of complicated hollow components from tubular or sheet blank material by means of water pressure. This method can achieve short development times, reduced number of operation steps, high precision, undisturbed material structure and increased uniform strength in the component.

This thesis presents the finite element simulation of the tube hydroforming process and optimization of the loading paths, (i.e., internal pressure and axial feed versus time).

ACKNOWLEDGEMENTS

I wish to express my gratitude to my co-advisors Dr. Farhang Pourboghrat and Dr. Erik D. Goodman for all the support, insight, guidance and expertise offered throughout my research. I would like also to thank ACD Associates specially Dr. David J. Eby and Ranny Sidhu for their advice and assistance during this research.

Also, I would like to thank the computational Mechanics Research Group for their support and assistance. Finally, I would like to thank my advisor Dr. Ronald C. Averill for his incredible amount of guidance, understanding and foresight throughout the duration of my thesis.

TABLE OF CONTENTS

LIST OF TABLES

LIST OF FIGURES

CHAPTER 1

INTRODUCTION

1.1 Introduction

Optimization problems are present in all disciplines and thus a wide range of goals exists. For example, the goals of manufacturing optimization problems can be to maximize product output, minimize material waste, minimize cycle time and maximize equipment use, etc. These goals, of course, coincide with the ultimate goal of business related optimization problems, which is to maximize profit. In the engineering field uncountable optimization problems exit. Of these, manufacturing process parameters optimization is the concern of the current study. In manufacturing process optimization goals are similar to other optimization problems. Many automobile and aerospace optimization problems are concerned with determining the design that minimizes weight while maintaining structural integrity and function.

Various techniques are used to solve optimization problems. Conventional techniques use gradient-based approaches, which have numerous limitations. Random search techniques are also limited to a class of practical problems that have small search spaces. A directed random search method such as a Genetic Algorithm (GA) is a multiple search method that can be an effective optimization approach to a broad class of problems. This technique is used to solve the process optimization problem in the current research.

1.2 Problem Definition

With the advancement in computer controls and high-pressure hydraulic systems, tube hydroforming (THF) process has become a viable method for mass production of structural components. Modern presses have independent control of axial feeding, internal pressure and counter pressure which allows the manufacturing of increasingly complex parts using the tube hydroforming process.

The emphasis on lightweight vehicle design also increases the requirements for parts produced using this technology. While hydroforming is new to the forming scene, it has quickly gained acceptance as a viable alternative to assembled stampings. Only a decade after its large volume applications, hydroforming is no longer being used only as a substitute for stampings. Many new vehicle platform designs are calling for the use of hydroformed components as the primary design option.

The metal forming industry is using finite element analysis (FEA) process simulation to develop successful tube hydroforming processes that would produce parts without defects. FEA can be conducted to predict most of the defects in the deformation zone such as buckling, wrinkling and bursting. These types of failure are caused by excessive axial feed and insufficient internal pressure.

To avoid the defects in THF, the applied internal pressure must be high enough to suppress buckling but not high enough to cause bursting. For this purpose FEA simulations are used. However, in conventional process simulation procedures, the user must estimate a pressure versus time, as input into the FEA programs. As a result many simulations must be conducted to obtain the desired results. Therefore, there is a need to develop a methodology to predict the loading paths (i.e., pressure and axial feeding versus time) necessary to hydroform a tubular part for a given geometry and material. In the current research a Genetic Algorithm is used to automatically optimize the process parameters. This technique is expected to reduce the number of simulations necessary to determine the "best" loading paths.

In the present work, a square shape die and a circular tube blank are considered. Displacement and internal pressure curves sought during the optimization are such that the circular tube can expand in to a square shape die to a maximum extent without bursting, buckling, and wrinkling. Consider a point 'P' on the tube as shown in the Figure (1.1). As the tube expands in the die, the distance 'U' traveled by the point increases.

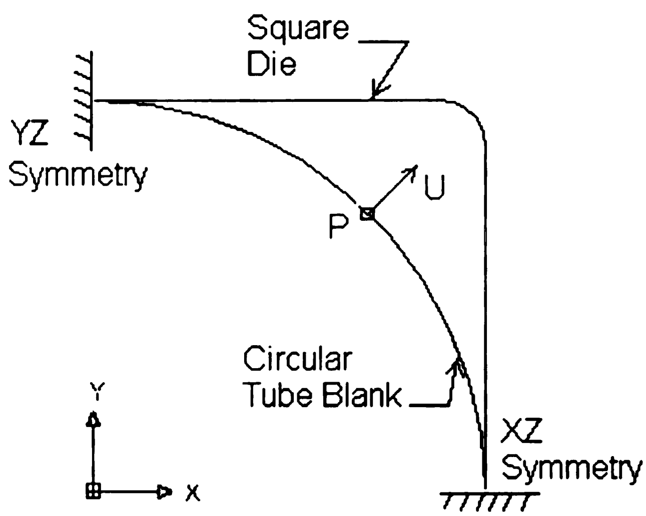

Figure (1.1) One-eighth model of the tube hydroforming optimization problem

Now the optimal value of the displacement and internal pressure is determined to maximize the distance 'U' without severe thinning and while satisfying the forming limit diagram (FLD). The FLD provides information about how much a particular metal can be deformed before necking occurs. The principal strains for each element of the hydroformed tube must lie under the major strain versus minor strain curve of forming limit diagram to avoid bursting the tubular blank within the square die for the optimal value of the loading path.

1.3 Literature Review

Olhoff and Taylor [6] present the basic concepts of structural optimization emphasizing the fundamentals. They discuss the features and elements involved optimization of both discrete and continuum structures, and also discuss the mathematical formulation of such problems. According to [6], fundamental structural optimization problems were of interest to the likes of Galileo (1638), J. Bernoulli (1687), Newton (1687), Lagrange (1770), and later to Saint-Venant (1864), Maxwell (1869), and Levy (1873).

Olhoff and Taylor [6] group design variables into six categories. Cross-sectional design variables are the first group. These variables refer to the properties of structural elements such as plate thickness and second moment of area, etc., which are typically assumed to be continuous but may also be discrete. Topological and configurational design variables describe the structural layout by specifying such things as the number and location of structural members and joints in a design. Shape design variables are variables, which are usually continuous and describe the structure shape. Material design variables describe material properties and are generally discrete. The final category is the support or loading design variables, which describe the loading and boundary conditions on the structure. This type of variable can be either discrete or continuous.

An optimal design problem can be termed discrete or continuous depending on the dependence of the design variables on the spatial coordinates of the problem. Design problems such as truss structures are discrete whereas plates and beams are often continuous.

In design problems certain constraints are imposed on all designs to help identify feasible designs. Olhoff and Taylor [6] divide constraints into two categories; behavioral and geometric constraints.

Behavioral constraints are, in general, non-linear constraints that can further be classified as equality or inequality. Equality constraints are, for example, equations of state and compatibility, which govern the structural response by placing limits on stress or deflection.

Geometric constraints can also be classified as equality or inequality. Geometric constraints place restrictions on the design variables due to manufacturing limitations or required appearance of the design.

To determine the "fitness" or "goodness" of a design, an objective function is used. The objective function is an expression given in terms of the design objectives, which have a value for each design or each point in the design space. While single-criteria optimization problems have been thoroughly studied, there are few realistic problems that contain merely a single objective to optimize. Multi-criterion optimization (MCO) problems involve the simultaneous optimization of several criteria and consequently are more difficult to solve.

Olhoff and Taylor [6] mention three of the better-known methods for solving MCO problems: weighted sum method, goal attainment or bound method, and the constraint method. A brief discussion of these methods will be given next. For explanation purposes c_i (D) will represent the criteria for design D, and the intent is to minimize with respect to D the vector $\{c_1, c2, c_3, \ldots, c_n\}$.

For the weighted sum method the problem is posed as:

$$\min_{D}\left(\sum_{i} w_i c_i\right) \tag{1.1}$$

Where $w_i \geq 0$ are weights specified by the designer based on the experience and judgement of the designer. This method determines D, which minimizes the weighted sum of all criteria.

In the constraint method the problem is given as:

$$\min_{D}(c_k) \quad \text{subject to } c_i - b_i \leq 0 \text{ (i=1,2,...n, i} \neq \text{k)} \tag{1.2}$$

Where the constraint bounds $b_i \geq 0$ are again specified by the designer.

The goal attainment or bound method defines the problem as:

$$\min_{D}(\xi) \quad \text{subject to } w_i c_i - \xi \leq 0 \text{ (i=1,2,...n)} \tag{1.3}$$

This method can be used to solve a min-max problem where for example the criteria c_i are identified with a maximum such as when the problem is stated as:

$$\begin{matrix}\min \\ \\ \max\end{matrix}\begin{pmatrix}\max(w_i c_i) \\ \\ i\end{pmatrix} \tag{1.4}$$

In this situation the weighted sum and constraint methods cannot be used.

Stadler and Dauer [7] first present a brief historical review of the field of multi-criteria optimization, tracing its origins to the area of economics. Stadler and Dauer [7] discuss optimization as finding Edgeworth Pareto optimal points (EP-points), which are named after the two economists Francis Ysidro Edgeworth and Vilfredo Pareto. EP-points are optimal or compromise points in a multi-criterion optimization problem.

Stadler and Dauer [7] outlined four steps involved in the solution of a multi-criterion optimization problem. First an appropriate mathematical model must be chosen, second a design set must be selected, third preferences are determined to allow the best design to be chosen, and finally the optimality concept or condition must be selected.

Stadler and Dauer [7] state the method of constraint approach is a good choice for solving multi-criteria objective problems. This approach is good since nearly any mathematical programming code can be used. Many standard approaches for analyzing multi-objective linear programs are based on the simplex algorithm, which generates a set of acceptable points from which the best design is chosen.

Finally Stadler and Dauer [7] outline examples of multi-criterion optimization problems from a survey they conducted. Two simple examples mentioned were the design of a simple arch structure, and of an elastic truss structure. More difficult and interesting optimization problems analyzed by Professor R. Statnikov of the Research Institute for Mechanical Engineering of the Russian Academy of Sciences in Moscow were also briefly mentioned. Statnikov applied his optimization methods to airframe and body design of the Russian space shuttle Buran. In this problem mass, structural rigidity, rib spacing, and cross-section shape were the design variables. This optimization effort gained a 300kg reduction in the tail section of the shuttle alone. Other work by Statnikov included design of the Russian truck ZIL. This problem contained 12 criteria.

Another example mentioned in [7] was conducted by H. Eschenauer, a Professor in the Laboratory for Structural Optimization at the University of Siegen, Germany. In his work Eschenauer solves the general optimal design problem for laminated conical shells with weight and deformations design criteria.

CHAPTER 2

DESCRIPTION OF TUBE HYDROFORMING PROCESS

2.2 Introduction

The hydroforming of tubes and hollow sections is by no means a new technique. The process has been around for decades and was used in the '70s [1] for the manufacture of designer sanitary appliances. The versatile technology available nowadays, with its high degree of reliability particularly in the field of control technology, has paved the way for numerous new hydroforming applications in various branches of industry in recent years.

The possibility of manufacturing ready-made precision parts in a wide variety of shapes and sizes which are both strong and lightweight means that this process will not only make its way in fields of application normally reserved for sheet metal forming, but also in fields which until now have been the exclusive domain of die casting and milling technology. The increasing use of hydroformed parts in the automobile industry is an impressive indicator of the importance of this promising technology, which is still very much in its infancy. It is mainly used in the automobile industry particularly for the manufacture of exhaust system components, engine cradle, radiator support, instruments panel support, side rails (Figure 2.1) and for producing industrial and sanitary appliances (Figure 2.2).

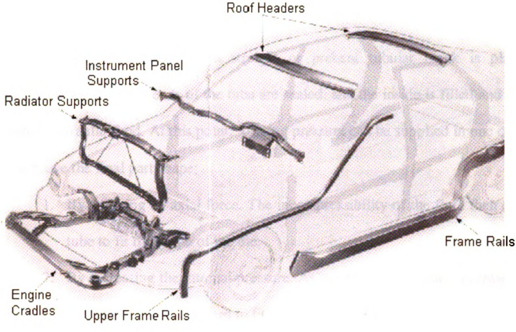

Figure (2.1) Applications in Automotive Industry [23].

Figure (2.2) Industrial and Sanitary Applications [4].

2.2 The hydroforming process

In tube hydroforming, a straight or prebent tubular blank is placed in an encapsulating die. The ends of the tube are sealed, and the inside is filled and pressurized with a hydraulic fluid. At this point, forming pressure can be supplied in one of four ways to achieve the final part shape:

1. By applying an axial force. The incompressibility of the fluid then expands the tube to fit the shape of the die.
2. By increasing the internal pressure. As the internal pressure increases, it bulges the tubular blank outward to fit the shape of the die.
3. By simultaneously applying an axial force and increasing internal pressure.
4. By applying an axial force first, and then, when the axial force fails to bulge the tubular blank completely to the final shape, increasing the internal pressure to complete the forming process.

Figure 2.3 illustrates the tube hydroforming process.

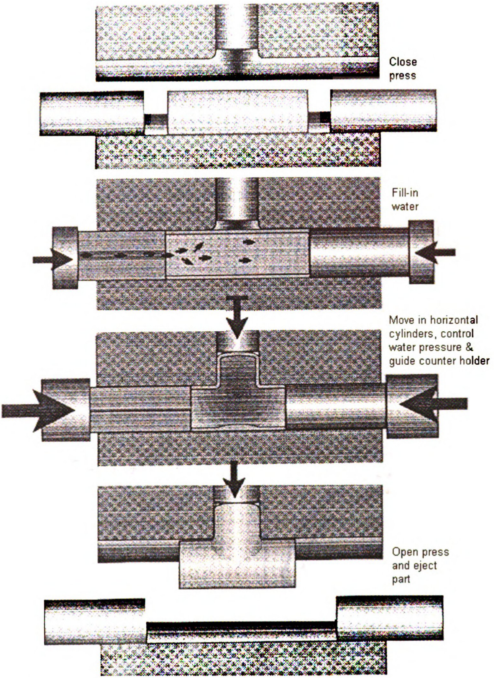

Figure (2.3) Tube hydroforming process [24].

2.3 Forming forces and Pressure

The principle of tube hydroforming requires the following three forces to complete the process (see Figure 2.4):

1. The closing force, F_s, is needed to close the tool.
2. The forming force, F_u, acts mainly on the ends of the tube and introduces axial compressive stresses into the tube wall while transporting the material into the forming zone.
3. The die force, F_w, acts in a direction perpendicular to the tube wall and also on elements branching off from the workpiece.

Initial internal pressure is generated by a pressure intensifier. During the process, pressure is applied to the inner profile of the tube, nearly allowing a free flow of material. When the internal pressure is low, the tube expands freely in die space without contact with the die surface. When the pressure is high, the tube comes in contact with the die surface and is deformed against the die profile. For this reason, the internal pressure and axial flow of the material must be closely controlled.

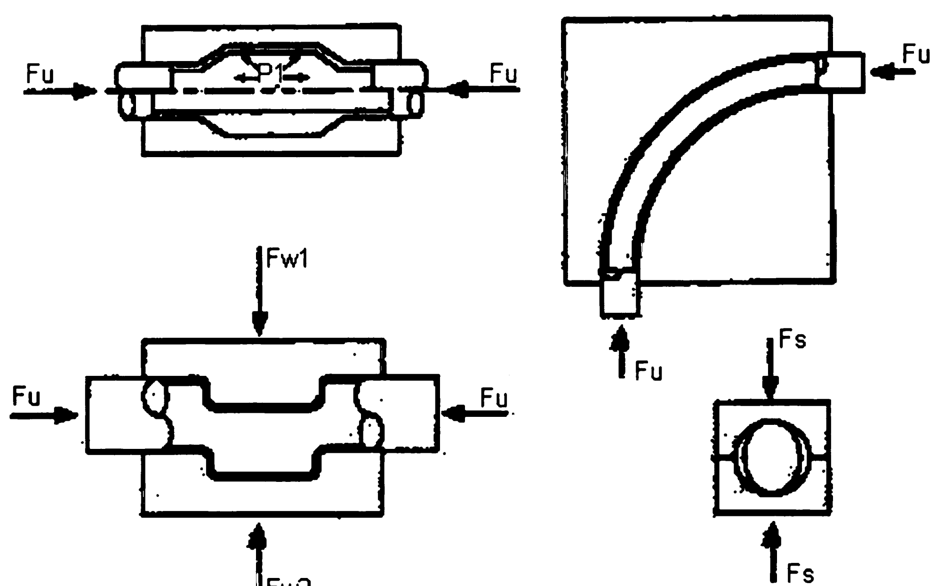

Figure (2.4) Pressure and forces in tube hydroforming [2].

2.4 Tube/Die contact

When the length of the tube in contact with the die is shorter, the required forming pressure is lower. When the contact length increases, the required forming pressure also increases [2].

When the ratio between the cross-sectional areas of the blank and the die is smaller, the contact length increases at a faster rate, causing a quicker increase in the forming pressure requirement [2]. Softer materials and longer tube blank lengths have the same effect. A larger cross-sectional area of the die results in a larger required forming pressure.

In simple terms, friction in the tube hydrofroming process can be described by the master-slave concept of friction [2]. This considers friction for the contact areas between the tool and the tubular blank. The coefficient of friction has a significant influence on the axial ram force necessary for the process.

2.5 Tube Hydroforming Systems

Currently there are three different tube hydroforming systems, low pressure forming, high pressure forming and pressure sequence or 2 pressure system. Each method forms the tube using different mechanisms, which will be described, in the following sections.

2.5.1 Low Pressure Forming

Low pressure forming occurs when the internal forming pressure is less than the pressure required to expand the tube along the corner radius of the final part. The internal pressure required to yield the tube in this area can be determined using hoop stress formulas. This technique can be used to form a tube with flat areas, large corner radii, and simple cross sectional designs. Figure (2.5a) shows an example of a simple cross section that can be formed by low pressure. However, difficulties such as pinching arise with the complex shapes, such as the form in figure (2.5b). Figure (2.6) shows the tube corner in a die with a large corner radius. The original wall thickness is maintained in the corner because the forming stress did not exceed the material yield strength.

Tube expansion during low-pressure hydroforming is possible, but it is limited to cross-section with a large radius. Tube expansion at the ends is possible with end feeding, but it must be done mechanically prior to hydroforming.

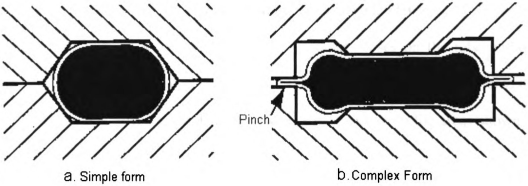

Figure (2.5) Low Pressure Forming System [3].

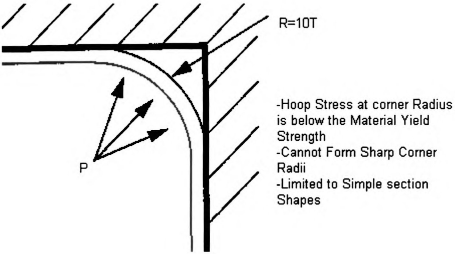

Figure (2.6) Forming Corner Radius, Low Pressure System [3].

2.5.2 High Pressure Forming

High pressure forming uses high internal pressure so that the tube hoop stress at the corner radius is higher than the material yield strength. In doing this, the tube fills the corner radius areas of the die by local stretching or expansion. Figure (2.7) shows the cross section of a tube in a complex shaped die. The die closes on the tube without pinching because the tube is smaller than the die cavity. As the higher pressures force the tube to the final shape, there is a reduction in tube wall thickness in the areas shown in Figure (2.8).

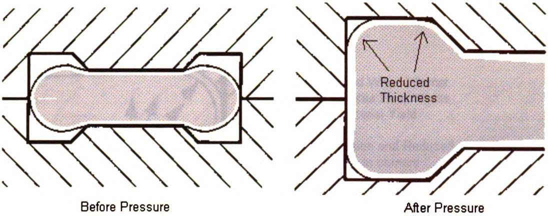

Figure (2.7) High Pressure Forming System [3].

Since high pressure causes significant friction between the tube and the die, the tube stretches significantly less in the flat areas than in the corner radius where material thinning occurs. The tube material must have high enough elongation to withstand the forming without bursting. Since press tonnage is proportional to forming pressure, and higher pressures require larger press sizes, a limitation occurs for larger structural parts.

Tube expansion (beyond forming the corner radius) is possible during high pressure hydroforming but it requires tube materials with high elongation and often times in-process annealing. Tube expansion at the ends using axial end feed in the forming die can also be employed.

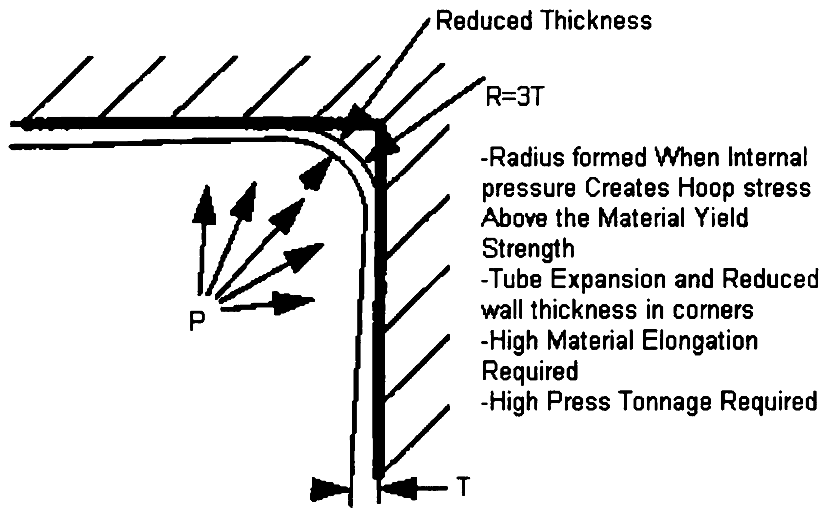

Figure (2.8) Forming Corner Radius, High Pressure Forming System [3].

2.5.3 Sequenced Forming Pressures

A pressure sequence system forms the corner radius by forcing the tube to flow into the corner without stretching or expanding the tube to fill the die cavity. The corner radius area is formed by exceeding the yield limit of the tube material in a bending mode, rather than a tensile mode as done in high pressure systems. This is accomplished by adding an additional pressure stage while the die is approaching the final closed position. Figure (2.9) shows a cross section of a die and tube during the pressure stages.

Figure (2.10) shows the die corner and how the pressure forms the radius in the tube by drawing the tube into the corner area. The free flow of metal in direction "F" allows an outside corner radius to be formed equal to 3 times metal thickness. During the first stage the pressures are low resulting in lower die friction, which is important for allowing the metal to slide along the die surface and into the corner area. The final formed tube is of uniform wall thickness around the circumference including the corner radii. After completion of the first stage a higher pressure is required to completely form the sides of the tube.

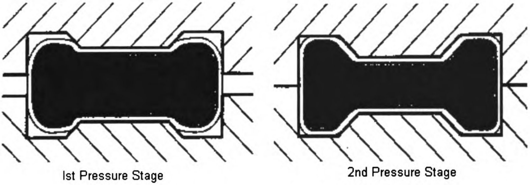

Figure (2.9) Sequenced Pressure Forming System [3].

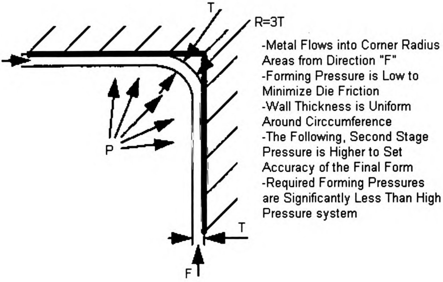

Figure (2.10) Forming Corner Radius, Sequenced Pressure Forming System [3].

Tube expansion during the hydroform process can be done during the second pressure stage. If required, expansion of the tube using end feed in the hydroform die is done as part of this stage. Tubes can also be mechanically expanded with end feed ahead of the hydroform die if there is a local indent or other complex form near the end of the final part.

Tube forming capability improvements have been developed using pressure stages, or a pressure sequence to improve metal flow in the forming dies. This multiple pressure sequence forms the tube into the complex shapes of the die cavity in a manner that reduces the natural pinching and buckling tendencies of traditional hydroforming. This process allows for the lower elongation values typical of aluminum and high strength steels, and also eliminates the need for in process annealing [3].

2.6 Failure Modes

The following failure modes [4] can occur when tubes with a straight longitudinal axis are being expanded as shown in Figure 2.11.

Buckling

Bursting

Wrinkling

Folding back

2.6.1 Buckling

There is a danger of buckling at the start of the process as a result of excessively high axial force (feeding) acting on the starting tube. This is a function of the tube parameters. The permitted buckling force at the start of the process can be estimated theoretically [5,8]. The danger of buckling persists beyond the initial stage of the process and lasts throughout the start-up phase. It is thus necessary to influence the process, through the process control, in such a way that the reduction in free tube length is coupled with a rapid increase in the section modulus of the tube cross-section [4].

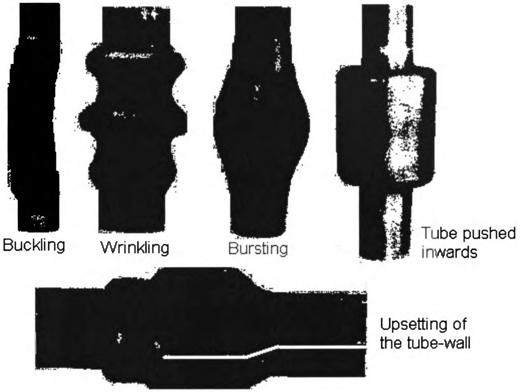

Figure (2.11) Failure cases that can occur during the hydroforming of rotationally symmetrical workpiece shapes [4].

2.6.2 Bursting

There is a danger of bursting once medium-level expansion has been attained ($d_1/d_0 > 1.4$) as a result of an excessively high internal pressure, where d_0 and d_1 represents the diameter of the tube before and after expansion. The bursting process is triggered by local constriction of the tube wall; the start of constriction is a major function of the starting wall thickness. These processes generally have a characteristic intermediate form of tube wall (in the form of a bulge towards the outside) associated with them [9]. The development of this intermediate form can be influenced via the process control; to avoid the danger of bursting it must be ensured that the tube wall is lying against the die by the start of constriction at the latest.

2.6.3 Wrinkling

Wrinkles that are symmetrical to the longitudinal axis can be eliminated by increasing the internal pressure in the final phase of the expansion process [4]. Additional wrinkles can, however, occur in the center of the workpiece, even in long expansion dies, as a result of excessively high axial force (feeding). The formation of these wrinkles can be avoided through an appropriate form of process control. It is also possible to estimate the danger of wrinkling by theoretical means, employing simplifying assumption [10].

2.6.4 Folding back

The danger of the workpiece folding back is conditioned both by the design of the die and by the expansion geometry and the tube parameters [11]. Folding back occurs when tubes are expanded in dies where tube wall material is forced into the die from tube holders. If this is done with thin walled tubes ($s_o/d_o < 0.05$), where s_o and d_o are thickness and diameter of the tube before expansion, then there is a danger of the tube folding back in areas of large-scale expansion ($d_l/d_o > 1.8$). In the case of tubes with thicker walls ($s_o/d_o > 0.1$), by contrast, there is a danger of the tube wall being compressed in the holder at lower expansion ratios already if the force required to feed further material into the expansion die is greater than the upset force. Figure 2.11 shows the transition from the holder to the expansion die, by way of example. The tube becomes compressed here and if further tube wall material is fed in from holder, material segregation can occur.

2.7 Advantages and Disadvantages

The advantages of the tube hydrofroming process are numerous. New and different materials can be used to produce parts. Lightweight materials with high strength-to-mass ratios, high-strength steels, and laminates can be used. Inexpensive, nonalloyed steels can also be substituted since, because of deformation, the tube material strain hardens and achieve higher strength than that of the initial tube.

Tube hydroforming allows complex part design because it can achieve deeper draws, varying thickness, varying cross sections, and severe shapes. These specific benefits are most important to part design:

1. Part consolidation means a single part replaces an assembly. We can reduce the number of parts using this technology.
2. Weight savings are significant as compared to conventionally formed parts (up to 40 to 50 percent). The savings are gained from the production of hollow parts, which have an inherently higher strength/weight ratio.
3. The stronger parts are due to a continuous weld versus the conventional spot welds. Strength is also increased by the inherent work hardening of the process. This allows for the use of thinner and less costly materials [12].
4. Surface and dimensional quality of part is improved. By providing a uniform strain distribution, the process has better shape control, reduced spring back, and less surface distortion. Outer dimensions are kept to exact tolerances with high precision.

In low volume production, the percentage of the final product cost accounted for by the tooling is significantly higher than in higher volume production [13]. The development and lead times are shorter than those for conventional methods of production, the prototype tooling costs less, and the material changes do not require new tooling.

The tube hydroforming process increases the formability of a material, which allows a reduction in the number of forming steps for a product, in turn reducing the number of tooling sets required.

The elimination of subsequent spot welding operations from the forming process creates significant savings in manufacturing costs. The capabilities of the process eliminate many secondary operations for additional savings.

This process also has drawbacks. In general:

1. The tube hydroforming process has a slow cycle time and, therefore, a low production rate. This limits the process to low-volume production or requires additional investment in equipment and tooling.
2. The dies in the tube hydroforming process require a high level of surface polishing. The frictional forces caused when the sheet blank contacts the die must be minimized as much as possible. Additionally, the surface quality of the die directly affects the surface quality of the final part's outer surface.

CHAPTER 3

TUBE HYDROFORMING SIMULATION AND OPTIMIZATION

3.1 Introduction

It is very cost-effective to make the right decisions early in a design process. Computer simulations are important as a tool to support these decisions. Nowadays, most components are simulated and their characteristics are studied. If their behavior appears to be non-satisfactory changes are made. The simulations are based on nominal data such as geometry, material parameters, residual stresses, etc.

The vehicle industry has established the technique of simulating the manufacturing process [14]. By dealing with sheet metal forming, the technique is highly developed and reliable enough to eliminate costly tools for test pressing. In other industries such as injection moulding and forging the technique was a tool used only in the academic world but today different software and packages are developed rapidly for commercial use.

Among the most common applications today is tool design and process optimization for the process industry. For a process like hydroforming this is of special significance. Designers don't have any designer's handbooks or deep knowledge in this area due to the relative immaturity of the process.

Various commercial Finite Element Analysis (FEA) software packages such as PAM-STAMP and LS-DYNA are capable of simulating the tube hydroforming processes. A successful tube hydroforming process requires proper combination of part design, material selection, and application of internal pressure and axial feeding. By using FEA methods, process parameters can be determined and then optimized using optimization software before manufacturing the dies and starting die try-out and process development. The use of automated design optimization software to optimize the process parameters in a hydroformed part has never been attempted to date. This is the goal of the present work.

3.2 Description of the geometry

Figure (3.1) illustrates isometric and front views of the tube hydroforming set up for the square expansion process. The major components of the equipment include two die halves with square cavities in the central area, and a circular tube blank.

The central section of the die cavity has square dimensions of 50.8 mm by 50.8 mm with corner radii 6.35 mm. The length of the cavity is about 50.8 mm. Circular tubes with diameter 50.8 mm and length 200 mm are used in the experiments and the simulations. The long sections on both sides of the central section are included to investigate frictional and axial displacement issues.

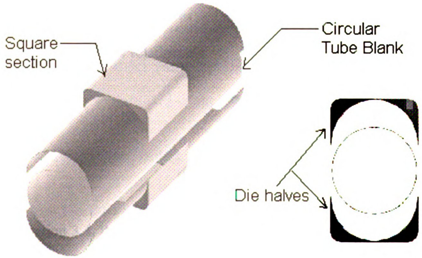

Figure (3.1) Tooling setup of square expansion process.

3.2.1 Tube Material

The tubes are made of Aluminum 6061 with T6 and T4 condition and wall thickness of 1.00 mm. Properties of this material are listed in Table 3.1.

Table 3.1 Material properties of the tube

Material	n-value	Modulus of elasticity (GPa)	Density (Kg/m^3)	Poisson's ratio	Yield Strength (MPa)	Tensile Strength (MPa)
Aluminum 6061 T6	0.0717	69	2700	0.33	235	282.77
Aluminum 6061 T4	0.1748	69	2700	0.33	118	216.47

3.2.2 Strain Hardening Exponent

The strain-hardening exponent (n-value) as listed in Table 3.1 is calculated using the Considere criterion [15].

$$\frac{d\sigma}{d\varepsilon} = \sigma \tag{3.1}$$

and using the power law relationship

$$\sigma = k\varepsilon^n \tag{3.2}$$

we have

$$\frac{d\sigma}{d\varepsilon} = nk\varepsilon^{n-1} = \sigma = k\varepsilon^n \tag{3.3}$$

From Equation 3.3, the following relationship between the maximum strain and n can be determined

$$\frac{n}{\varepsilon} = 1 \tag{3.4}$$

The true stress at the maximum load is also known from [15]

$$S_u = k\left(\frac{n}{e}\right)^n \tag{3.5}$$

Where e = 2.7183 is the base of the natural logarithm.

Using Equations 3.2 and 3.5 and assuming that $\sigma = \sigma_y$ when $\varepsilon = 0.002$, it is possible to obtain the following equation for calculating n.

$$n = \frac{\ell n(\sigma_y) - \ell n(S_u)}{\ell n(0.002) + \ell n(e) - \ell n(n)} \tag{3.6}$$

The Equation 3.6 can be solved for n, iteratively, for known values of the ultimate tensile strength, S_u, and the yield stress, σ_y, of the material. From the uniaxial tensile test for 6061-T6 Aluminum we get a value of $S_u = 282.77$ MPa at the ultimate load. Using the 0.2% offset condition we also calculate the yield stress to be $\sigma_y = 235$ MPa.

By substituting for these values into equation 3.6, we get the following n-value

$$n = 0.0717$$

The strength coefficient (k) was then calculated from Equation 3.2.

$$k = 366.93 \text{ Mpa}$$

3.2.3 Stress-Strain relationship

Table 3.2 shows the true stress and plastic strain data for Aluminum 6061-T6 obtained through tensile test of the material [20]. Based on this data Figure 3.2 shows the true stress plastic strain relationship.

Table 3.2 True Stress Plastic Strain data for Aluminum 6061-T6 [20]

Plastic Strain	True Stress (MPa)
.000000000E+00	.235000000E+03
.553623000E-02	.239000000E+03
.848696000E-02	.242400000E+03
.114594000E-01	.244300000E+03
.144225000E-01	.246850000E+03
.173916000E-01	.248980000E+03
.203617000E-01	.251040000E+03
.233313000E-01	.253140000E+03
.263004000E-01	.255270000E+03
.292706000E-01	.257330000E+03
.322416000E-01	.259330000E+03
.352130000E-01	.261300000E+03
.381880000E-01	.263030000E+03
.411638000E-01	.264700000E+03
.441406000E-01	.266300000E+03
.471213000E-01	.267630000E+03
.500984000E-01	.269210000E+03
.530804000E-01	.270450000E+03
.560617000E-01	.271740000E+03
.590464000E-01	.272800000E+03
.620317000E-01	.273810000E+03
.650174000E-01	.274800000E+03
.680030000E-01	.275790000E+03
.709904000E-01	.276660000E+03
.739794000E-01	.277420000E+03
.769701000E-01	.278060000E+03
.799604000E-01	.278730000E+03

.829512000E-01	.279370000E+03
.859442000E-01	.279850000E+03
.889372000E-01	.280330000E+03
.919307000E-01	.280780000E+03
.949248000E-01	.281190000E+03
.979207000E-01	.281470000E+03
.100917000E+00	.281760000E+03
.103912000E+00	.282070000E+03
.106909000E+00	.282290000E+03
.109906000E+00	.282460000E+03
.112905000E+00	.282580000E+03
.115903000E+00	.282700000E+03
.118902000E+00	.282770000E+03
.136902000E+00	.282770000E+03

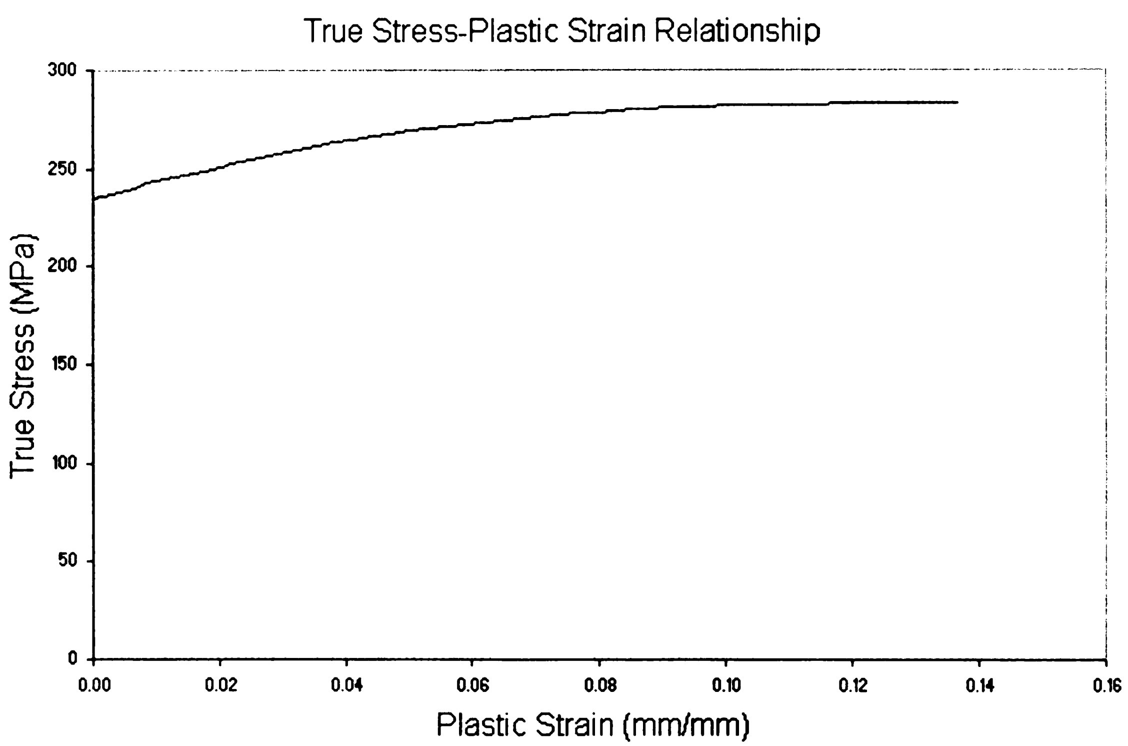

Figure (3.2) Experimentally obtained stress-strain relationship [20].

The tool geometry has been created in I-DEAS master series [21] and imported into DYNAFORM-PC [22] on an IGES file. DYNAFORM-PC [22] is a pre- and post-processor for LS-DYNA [17]. Other geometries like tube blank and punch has in a similar way been created directly in I-DEAS and imported from an IGES file.

The commercial program LS-DYNA from Livermore Software Technology Corporation has been used to analyze the hydroforming process. The program is an explicit FEA program and solves nonlinear problems. In comparison to an implicit FEA program the explicit is much faster due to the advantage of avoiding matrix inversions and it also requires less data storage [16].

3.3 Simulated Tube

The tube has been modeled with shell elements. In most explicit codes, shells are assumed to be composed of a number of laminae, with each lamina satisfying the plane stress assumption. One constitutive evaluation is performed for each lamina, yielding a potentially complex through-thickness stress distribution. Numerical integration with one integration point in each lamina is used to compute the resultant forces and moments on the shell. In LS-DYNA, this integration may use from two to five pre-defined points through the thickness, or any number of points in a user-defined integration rule. Fewer points yield sufficient accuracy in regions of predominantly membrane behavior, while more points improve accuracy when bending effects and plasticity are combined [18]. In this case the Belytschko-Tsay [17] element with five integration points through the thickness has been used.

The tools for this simulation are modeled as rigid. By modeling the tooling as rigid in the finite element model, a fine mesh may be used to accurately resolve the details of tooling geometry (such as radii of curvature) without significantly increasing the cost of the analysis. Elements using the rigid material don't affect the time step, and therefore rigid element sizes may be selected solely on the basis of accurately representing the tooling shape.

The material model used is a transversely anisotropic elastic plastic model. This is material 37 in LS-DYNA [17].

The formability of tube material is often evaluated from strain analysis through the Forming Limit Diagram (FLD), which represents the relationship between the limiting major and minor principal strains in the plane of the strained tube.

Table 3.3 shows the FLD data for $n = 0.0717$ and thickness of 1.00 mm for Aluminum 6061-T6. Figure 3.3 shows the Forming Limit Diagram based on FLD data listed in Table 3.3 for the same material.

Table 3.3 FLD data for Aluminum 6061-T6

Minor Strain (mm/mm)	Major Strain (mm/mm)
-.494296300E+00	.700827800E+00
-.446287100E+00	.642684000E+00
-.400477600E+00	.585192700E+00
-.356674900E+00	.528683500E+00
-.314710700E+00	.473534200E+00
-.274436800E+00	.420171100E+00
-.235722300E+00	.369068400E+00
-.198450900E+00	.320743700E+00
-.162518900E+00	.275750900E+00

-.127833400E+00	.234667600E+00
-.943106800E-01	.198078800E+00
-.618754000E-01	.166556200E+00
-.304592100E-01	.140633600E+00
.000000000E+00	.120780400E+00
.295588000E-01	.146086300E+00
.582689100E-01	.166843000E+00
.861777000E-01	.183938500E+00
.113328700E+00	.198065200E+00
.139761900E+00	.209770100E+00
.165514400E+00	.219489900E+00
.190620400E+00	.227575800E+00
.215111400E+00	.234312500E+00

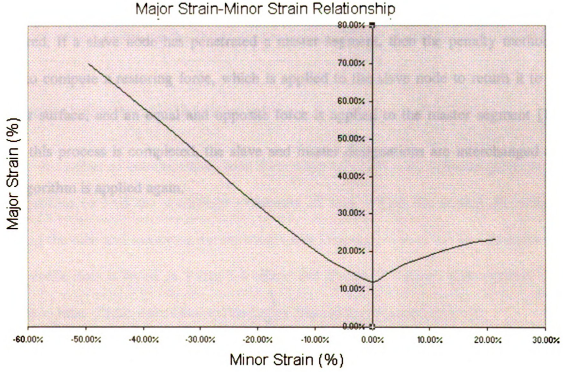

Figure (3.3) Forming Limit Diagram for Aluminum 6061-T6.

The tube material is assumed to be uniform throughout the thickness. The friction coefficient is also assumed to be a constant value of 0.03 throughout [2]. One-eighth part of tube is considered in the FEM model (due to existing symmetries) to reduce the simulation time as shown in Figure 3.4.

The mesh has been defined with adaptive characteristics. This improves the curvatures in the small radii of the tool where it is needed the most instead of defining small elements all over the tube.

In order to avoid properly account for blank/tool contact in the hydroforming process, the blank is modeled as a slave surface and tooling as the master surface. The two contact surfaces are individually described by a collection of contact segments, which are simply element faces on the contact surface. For each slave node, the contact algorithm first searches through the master segments to determine if any penetration has occurred. If a slave node has penetrated a master segment, then the penalty method is used to compute a restoring force, which is applied to the slave node to return it to the master surface, and an equal and opposite force is applied to the master segment [18]. Once this process is completed, the slave and master designations are interchanged and the algorithm is applied again.

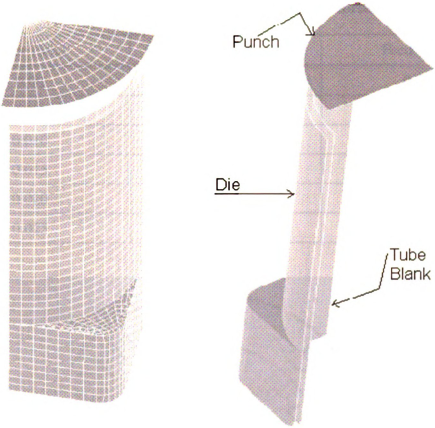

Figure (3.4) One-eighth model of tube hydroforming simulation, meshed and unmeshed.

3.4 Results before using optimization software

A number of iterations have been done using LS-DYNA for different pressure and feed profiles to find the maximum expansion of tube within the square die without bursting the tube and satisfying the Forming Limit Diagram. One of the best pressure and feed profile data is listed in Table 3.4 below and Figure 3.5 shows their relation with respect to time. These were obtained through a manual optimization process.

Table 3.4 Pressure and feed verses time for tube hydroforming simulation

Time (Sec)	Pressure (Mpa)	Feed (mm)
0.00	0.00	0.00
0.005	9.5	0.5
0.010	9.5	3.5
0.015	10.5	3.5
0.020	10.5	6.5
0.025	11.5	6.5

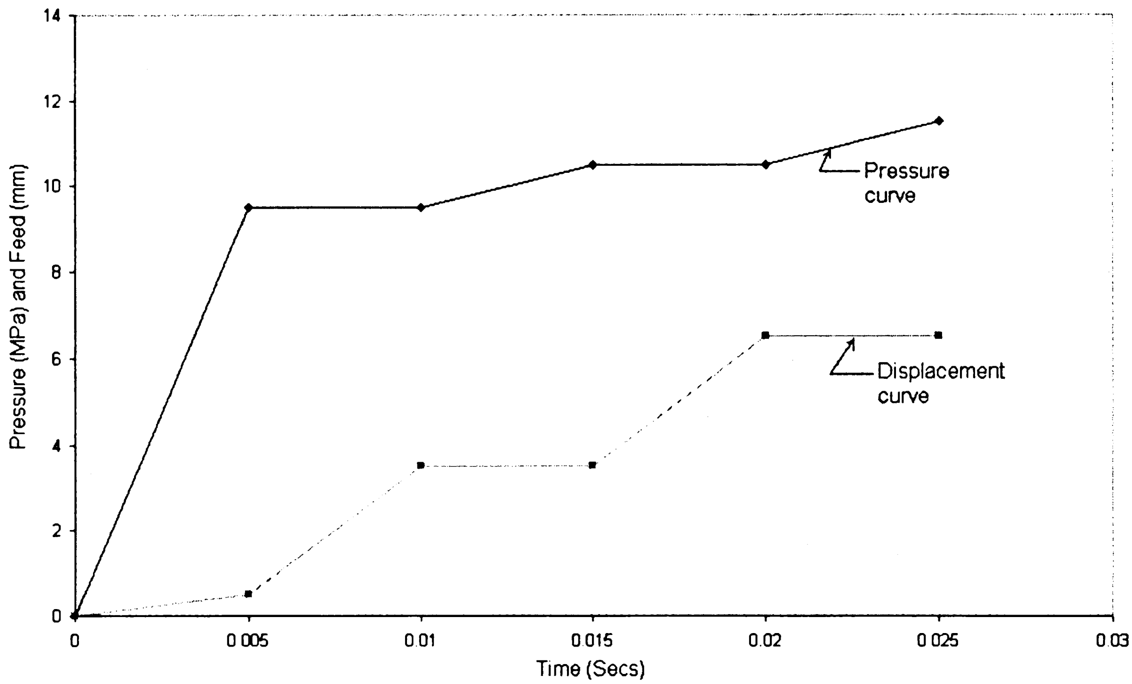

Figure (3.5) Internal Pressure and Feed versus Time Relationship.

At time step 0.01448 sec, internal pressure is about 10.3 Mpa and feed is about 3.5 mm. The maximum expansion of tube before failure at above pressure and feed rate is illustrated in Figure 3.6. Figure 3.6 shows that the tube expands up to 14.8 mm radius. A slight increase in pressure above 10.3 Mpa results in the bursting of the tube at the given feed rate.

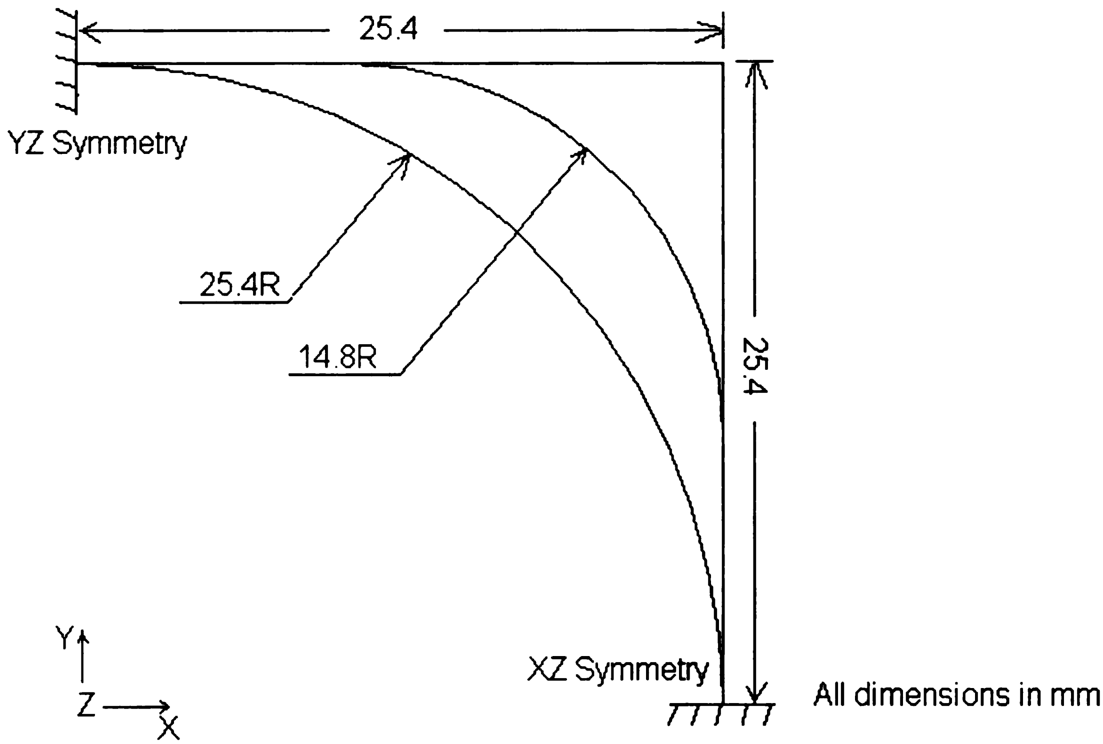

Figure (3.6) Maximum radius obtained for the deformed tube before failure.

Principal strains for the deformed tube lie within the Forming Limit Diagram as shown in Figure 3.7. Figure 3.8 shows the thickness plot and Figure 3.9 shows the von Mises stress plot for the tube before failure.

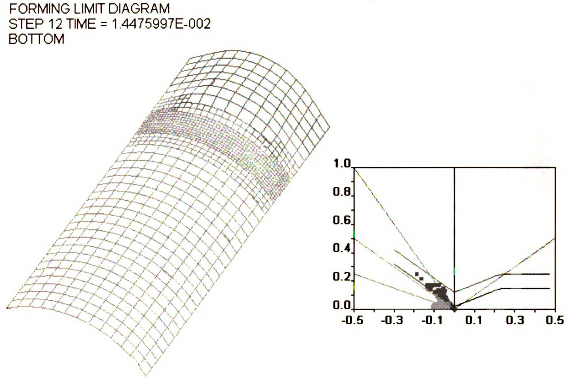

Figure (3.7) Forming Limit Diagram for the deformed tube before failure.

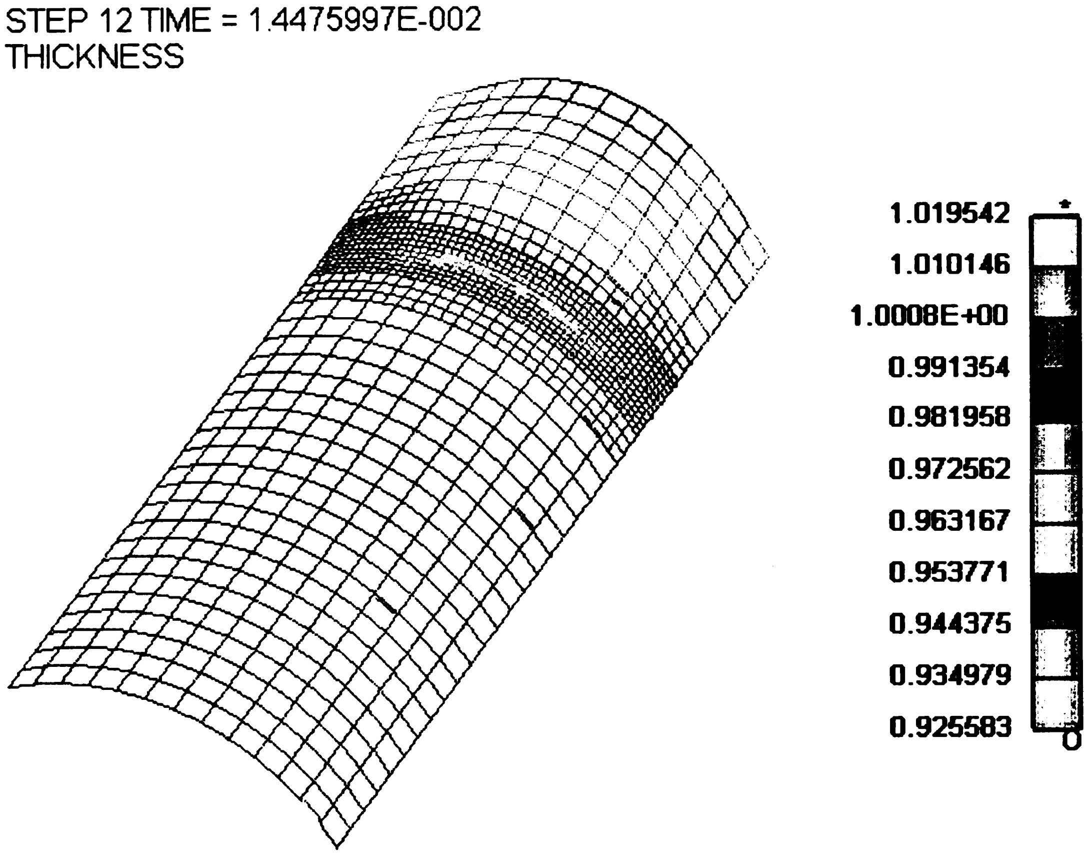

Figure (3.8) Variation in thickness for the deformed tube.

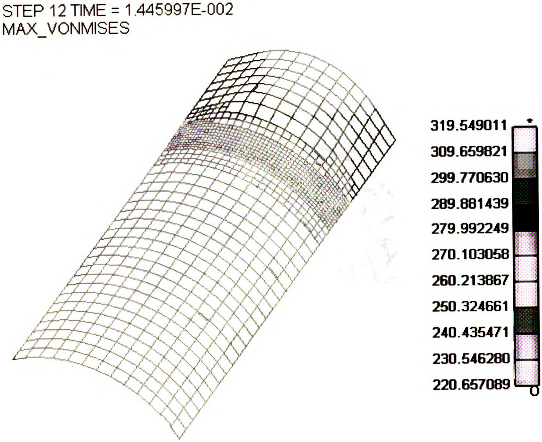

Figure (3.9) Von Mises Stress plot for the deformed tube.

3.5 Experimental Validation

To validate the simulation results, Aluminum 6061 with T6 condition tube has been tested experimentally in a Michigan State University research lab using the tube hydroforming press as shown in Figure (3.10).

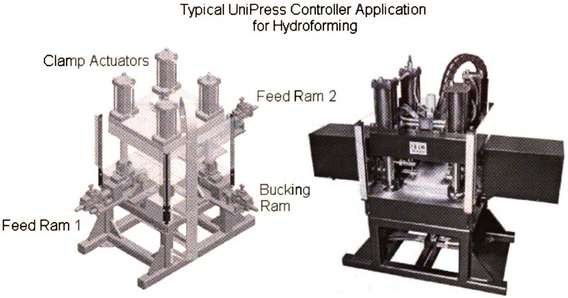

Figure (3.10) Experimental set up for tube hydroforming [25].

Figure (3.11) shows the Forming Limit Diagram for the simulated tube without rupture at time 0.01447599 sec and at a pressure of 10.3 Mpa with feed of 3.5 mm and Figure (3.12) shows rupture in the simulated and experimentally tested tube as the pressure increases with the same feed rate. Figure (3.13) shows the shape comparison between the simulated and experimentally tested tube.

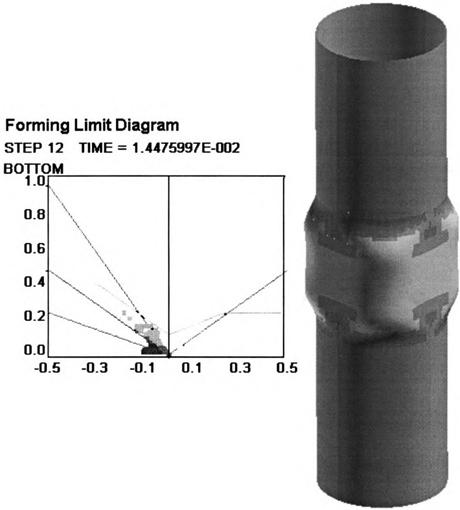

Figure (3.11) Forming limit diagram for the simulated tube before failure, full view.

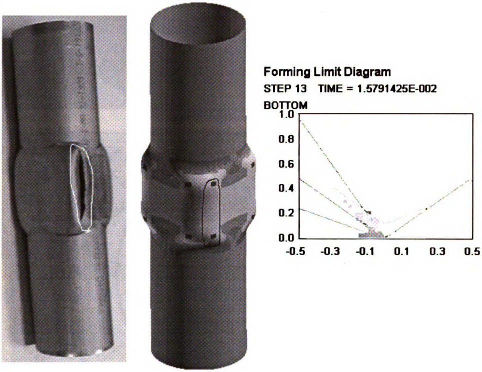

Figure (3.12) Cracks in experimental and simulated tubes.

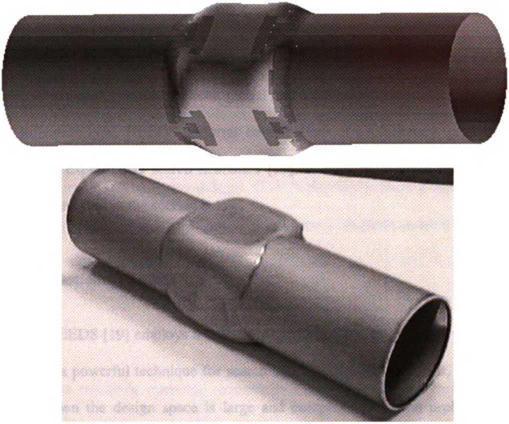

Figure (3.13) Simulated and experimentally tested tube shape comparison.

Now the optimization software HEEDS (Hierarchical Evolutionary Engineering Design System) [19] is used to find the optimal pressure and feed rate profiles for the maximum expansion of the tube within a square die before rupture.

3.6 Optimization using HEEDS

The optimization problem in the current research is classified for HEEDS as type one, which compromises between global and local search techniques. For this problem classification type, HEEDS performs combinations of evolutionary, gradient based, and design of experiments search heuristics [19]. A brief description of search techniques used is presented in the section below.

3.6.1 Evolutionary Search

HEEDS [19] employs a Genetic Algorithm (GA) to perform evolutionary search. A GA is a powerful technique for search and optimization problems, and is particularly useful when the design space is large and complex. The main problem with using a simple GA is the potentially large number of design evaluations required to obtain a set of satisfactory solutions. HEEDS reduces the number of evaluations required to obtain a set of satisfactory solutions by hierarchically decomposing a problem with multiple agents that represent the problem in various ways, while combining efficient local search methods (automated design of experiments, nonlinear sequential quadratic programming, and simulated annealing).

A GA is a search procedure based on the mechanics of natural selection. Specific knowledge is embedded in a chromosome (or design vector), which represents a possible design with a set of values of all the design variables. The number of choices per design variable determines the fidelity (or resolution) of each design variable.

A GA creates and destroys designs during a process that involves decoding each chromosome, evaluating its satisfaction of constraints and its performance relative to the objectives, and then allowing a simulated "natural selection" to determine which designs are eliminated and which survive to generate other, derivative designs. Designs that perform well (relative to constraints and objectives) have a higher probability of surviving to influence future designs (their "offspring"). During reproduction, the two genetic operators commonly modeled that produce new chromosomes (or design vectors) are called crossover and mutation.

3.6.1.1 Crossover

The crossover operation (sometimes also called "recombination") forms a new solution by combining parts of two existing solutions. A high crossover rate (fraction of population replaced by crossover during one generation of reproduction) will produce many new designs in each generation, but will also have a high probability of disrupting (and potentially losing, at least temporarily) higher-performance designs already found, and requires more evaluations of constraints and objectives in each generation (which are typically the most costly computing operation in the entire problem).

3.6.1.2 Mutation

Mutation is a reproduction operation that produces a new solution from a single existing solution, through any of several ways. Mutation can change the value of one design variable, or of many simultaneously, and can change them in uniform random ways, or distributed normally, for example, around the current values of the design variables. Mutation helps maintain diversity and reduces the possibility of premature convergence (the tendency of a set of solutions to come to closely resemble each other, thereby making it difficult for crossover to generate solutions that differ very much from the current set).

A set of co-existing designs defines a population, while successive populations are termed generations. That is, each period during which a set of existing solutions are evaluated, then used with natural selection, crossover, and mutation to generate a new set of solutions, is called a generation. A large population typically contains more genetic diversity (i.e., more different values of design variables), that typically improves the ultimate results of the GA search. However, the more new individuals created in each generation, the more computer time must be spent evaluating the constraints and objectives of the new individuals, so there is a tradeoff that must be made.

Figure 3.14 displays the structure of a simple GA. The simple GA begins by creating a single initial population, wherein chromosomes (vectors of design variable values) are randomly created. At this point the performance (constraint satisfaction and objective values of each design is evaluated. Biased by the evaluations obtained, the GA uses unary (mutation) and binary (crossover) operators on these designs to create another population. This population probabilistically maintains the previously high performing designs while discarding poorly performing designs. New population members are evaluated, and then additional rounds of generation and selection are performed. This is repeated until satisfactory solution(s) are obtained. Incorporating these processes in a computer algorithm produces an algorithm that solves problems in a manner reminiscent of natural evolution.

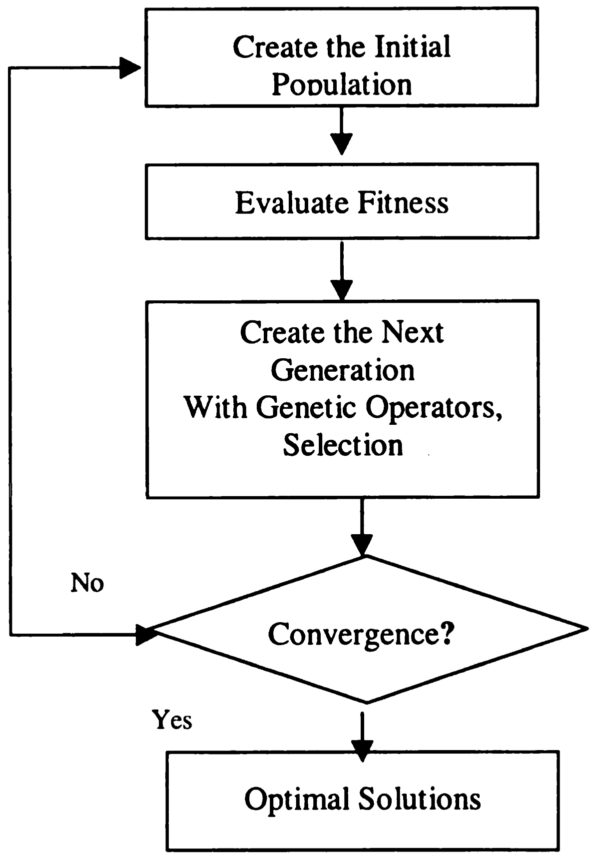

Figure (3.14) The structure of a simple Genetic Algorithm [19].

3.6.1.3 Representation of Design Variables within a Chromosome

A chromosome of "p" design variables (x_i) can be represented in vector form as: $\{x_1, x_2, x_3, \ldots\ldots, x_p)$. Each design variable represents a field (or locus) on the chromosome (or design vector). The number of choices per design variable will define its resolution, or fidelity. If a coarse representation of a continuous design variable is sought, then the field size of the continuous design variable should have a small number of choices between the lower and upper bounds of the design variable. A large number of choices between the lower and upper bounds of a continuous design variable can be defined to refine the representation of the continuous design variable. Each design variable (field) on the chromosome can have an independent field size. If a design variable is truly discrete in nature, then the field size of the discrete design variable should be set at the number of choices in the discrete set.

3.6.1.4 Initial Population Generation

First, a GA typically performs random initialization, then evaluation of the initial population. The GA stochastically creates a population of chromosomes composed of a randomly chosen design variable at each field. A performance measure (or fitness) is assigned to each design (or individual) based on the degree to which it satisfies the problem's constraints and extremizes its objectives.

3.6.1.5 Selection

The next process the GA must perform is selection. The selection mechanism for a GA is simply the process that favors the selection of high-performance individuals to be placed in the "mating" pool of individuals to undergo crossover, mutation, and/or unaltered survival to the next generation. The performance measure (or fitness function) provides a means of comparing individuals and the selection process determines how the individuals are compared. Selection mechanisms determine which chromosomes are placed in the mating pool. The mating pool is comprised of the individuals from which the next generation will be created. Selection is the GA search catalyst that works by mimicking natural selection.

3.6.1.6 Definition of Performance

The "goodness" of each design is represented with a single scalar value called the performance measure. The performance measure is a composite of a number of subsidiary measures, a set of objectives (each of which may be targeted for maximization or minimization) and a set of constraints, for which violations are to be minimized. The constraints enter into the performance according to the penalty method, which gives them no influence so long as they are satisfied, but gives them increasing importance to whatever extent they fail to be satisfied. Within any single agent, to evaluate the performance measure (or fitness) of a design, the objective and constraint functions are normalized, weighted, and aggregated:

$$P = \sum_{i=1}^{Nobjs}\left(R1_i \frac{f_{oi}}{|n_i|} + R2_i \left(\frac{f_{oi}}{|n_i|}\right)^2 \right) - \sum_{i=1}^{Ncons} C\left(P1_i \frac{|f_{ci} - t_i|}{|t_i|} + P2_i \left(\frac{f_{ci} - t_i}{|t_i|}\right)^2 \right) \tag{3.7}$$

Where P is the performance measure, Nobjs is the number of objectives, and Ncons is the number of constraints. $R1_i$ is a constant used to linearly reward a design's performance due to extremizing of the i^{th} objective function. $R2_i$ is a constant used to quadratically reward a design's performance due to extremizing of the i^{th} objective function. The

i^{th} objective function (f_{oi}) is normalized by the absolute value of n_i. $P1_i$ is a constant used to linearly penalize a design's performance for violating the i^{th} constraint function. $P2_i$ is a constant used to quadratically penalize a design's performance due to the violation of the current constraint function. The i^{th} constraint function (f_{ci}) is normalized by the absolute value of its target t_i. If the constraint is satisfied, C is set to zero; if the constraint is violated, C is set to unity.

3.6.2 Nonlinear sequential Quadratic Programming

Nonlinear Sequential Quadratic Programming (NLSQP) is a gradient-based search technique that efficiently solves an explicit set of optimization problems. NLSQP is used to solve deterministic, unimodal, convex, first-order differentiable objective and constraint functions. NLSQP will quickly converge to the global optimum if the objective and constraint functions are deterministic, have first-order continuity, and satisfy convexity criteria. NLSQP will quickly converge to a local optimum if the objective and constraint functions are deterministic, have first-order continuity, but fail to satisfy convexity criteria.

NLSQP is a single point search technique that applies gradients of the objective and constraint functions (with respect to continuous design variables) to define a search direction to improve the performance of the current design. Since most simulation packages do not compute analytical gradients of objective and constraint function, the calculations of gradients are approximated through numerical differentiation. The numerical differentiation is implemented within HEEDS with a forward differencing scheme.

3.6.3 Automated Design of Experiments

HEEDS does type-zero Design of Experiments (DOE) by reusing previously computed evaluations to construct response surfaces and then using nonlinear sequential programming to search, from an initial design, for designs projected to have improved performance.

3.6.3.1 Type-Zero Design of Experiments

HEEDS conduct type-zero DOE about an initial "starting point" design by: 1) collecting a training set of previously evaluated designs based on simple normalized distance criteria measured relative to the starting point, 2) fitting linear and quadratic surfaces (in a least squares sense) to the training set, to approximate the various constraint and objective functions in the vicinity of the starting point design, 3) applying NSQLP using the approximated objective and constraint functions with their least squares polynomial surfaces, and 4) automatically updating the training set for the next DOE.

The training set for type-zero DOE is based on a simple normalized absolute distance metric, and is collected from all previous design evaluations of identical representation and performance type:

$$d = \frac{1}{N}\sum_{i=1}^{N}\frac{|X_i - T_i|}{R_i} \tag{3.8}$$

Where N is the number of design variables, X_i is the starting point's i^{th} design variable, T_i is the i^{th} design variable of design under consideration to be included in the training set, and R_i is the resolution of the i^{th} design variable. The minimum distance is zero (the starting point) and the maximum distance is unity. All designs that have an absolute normalized distance less than or equal to a prescribed maximum distance and greater than or equal to a prescribed minimum distance will be included in the training set of the DOE.

3.6.4 Simulated Annealing

Simulated annealing (SA) is based on the statistical mechanics of annealing solids. To understand how such an approach can be used as an optimization tool, one must consider how to coerce a solid material into a low energy state. Annealing is a process typically applied to solid materials to force the atomic structure of the material into a highly ordered state. If a material is brittle in nature, its atomic structure is not in an ordered state. If the material is heated to a high temperature, the atomic structure shakes violently, allowing for alternate, more ordered, energetically favorable, atomic states. In an annealing process, a material is heated to a high temperature and slowly cooled. If the material is cooled suddenly, the atomic order is locked into a random unstable state. If the material is cooled slowly, the atomic structure tends to fall into relatively stable configurations for each temperature. As the temperature is slowly dropped, the material state will eventually stabilize into a highly ordered state.

Implemented as an algorithm, SA begins with an initial design, a starting temperature, an ending temperature, a total number of temperatures to consider, and the number of iterations per temperature. As coarsely depicted in Figure (3.15), SA begins with an initial design at a specified starting temperature. Then, the initial design is subjected to a specified number of random perturbations based on the starting temperature. If the staring temperature is close to unity, the perturbations are large, yielding a broad search relative to the initial design. If the starting temperature is small, the perturbations are small, yielding a localized search about the initial design. If a perturbation locates a better design, the initial design is updated with the improved design. Once the number of iterations at that temperature is exceeded, the temperature is decreased and the perturbation process is iterated. This process of decreasing the temperature and iterating repeats for the total number of temperatures. The ending temperature should be small, and will result in more localized search than the starting temperature.

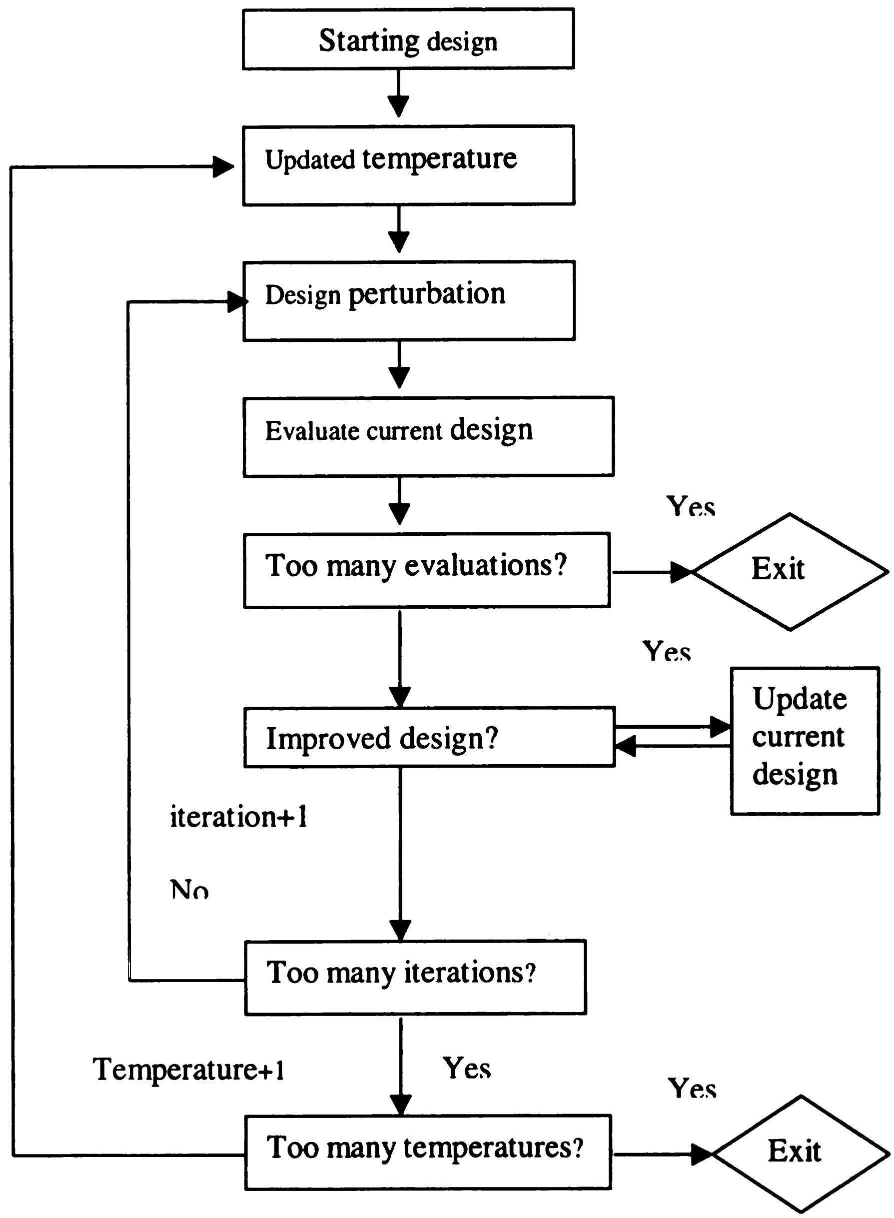

Figure (3.15) Flow chart for simulated annealing [19].

3.7 Results after using optimization software

HEEDS is used to optimize the process parameters; the recommended eight procedural steps for HEEDS input are followed. A dynamic link library was written to perform the objective and inequality constraint function evaluations. This problem does not require design criteria template files to be created, so the first step to 'Define a Baseline Design' is not required. For this problem, the objective function will be maximized while satisfying the constraint on the forming limit diagram. This is done in the second step that is to 'Define the Design Criteria'. The design criteria are specified in a Performance file with an id of 1. The third step is 'Define the Design Variables'. HEEDS requires the definitions of static parameters of all possible design variables to be declared in the 'Definition.in' file. For this problem, we do not need to define this file because we use user-defined variables. These variables are declared in the 'Representation1.in' file. In the fourth step 'Represent the Design Variables', a collection of design variables to be varied by an agent is defined in a 'Representation1.in' file. The fifth step is 'Define the Agent Topology'. A single agent is applied to this problem. The 'Topology.in' file defined all of the agents in the HEEDS project. Each agent is assigned a representation id, a performance id and the number of neighbors for the agent.

The search parameters file is input on the HEEDS command line. This is done in the sixth step, 'Define the Search Parameters'. The seventh step is, ' Execute the Optimization Run' in which HEEDS executes the problem. HEEDS terminates after evaluating the specified number of cycles. Upon termination, the designs found in the HEEDS00.dat and HEEDS00.plot files can be recovered, and reevaluated through post-processing. This is done in the last eighth step 'Post-Process the Solution(s)'.

HEEDS gets the strain components information as output from LS-Dyna and calculates the principal strains, compares calculated principal strains with the principal strains of the forming limit diagram for the tube material Aluminum 6061 with T6. After satisfying the forming limit diagram, maximize the tube expansion within a square die without rupture and then find the optimal value for the design variables i.e. pressure versus time and feed versus time in step wise linear fashion. At the end of generation 6 and evaluation 224, the best design is found for the process parameters. Table (3.5) shows the optimized pressure and feed rate data and Figure (3.16) illustrates the respective profiles for the process parameters. Figure (3.17) represents the maximum expansion of the tube in a square die without failure, after optimization.

Table (3.5) Internal Pressure and Feed versus Time (Generation=6, Evaluation=224)

Time (sec.)	Feed (mm)	Internal Pressure (Mpa)
0.000	0.00	0.00
0.005	4.75	9.00
0.010	4.75	10.13
0.015	6.50	12.40
0.020	6.50	21.08
0.025	6.50	22.09

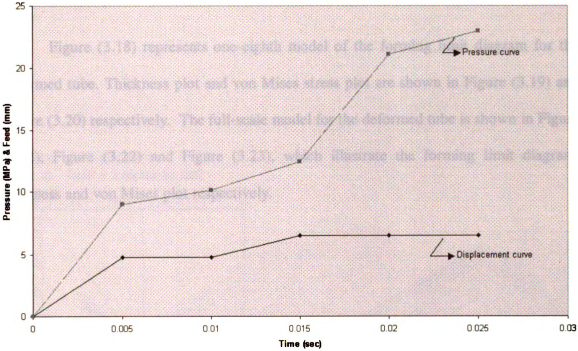

Figure (3.16) Internal Pressure and Feed versus Time Relationship (Gen=6, Evl=224).

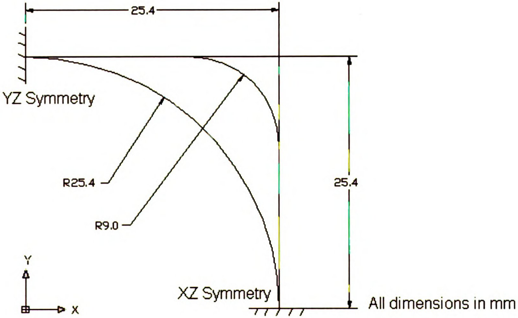

Figure (3.17) Maximum radius obtained for the deformed tube before failure, after optimization by HEEDS.

Figure (3.18) represents one-eighth model of the forming limit diagram for the deformed tube. Thickness plot and von Mises stress plot are shown in Figure (3.19) and Figure (3.20) respectively. The full-scale model for the deformed tube is shown in Figure (3.21), Figure (3.22) and Figure (3.23), which illustrate the forming limit diagram, thickness and von Mises plot respectively.

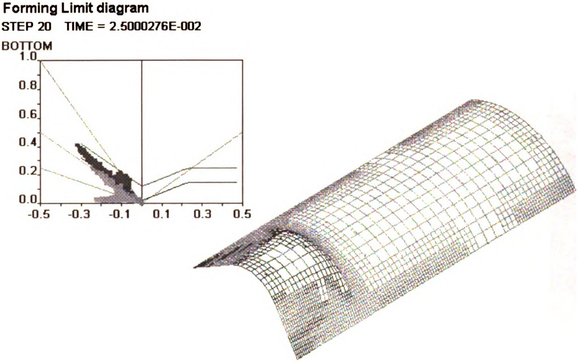

Figure (3.18) Forming Limit Diagram for the deformed tube before failure, after optimization.

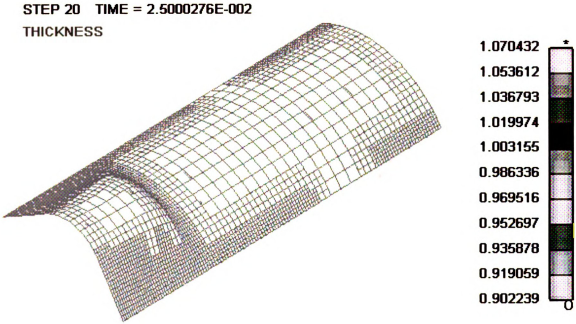

Figure (3.19) Thickness plot for the deformed tube before failure, after optimization.

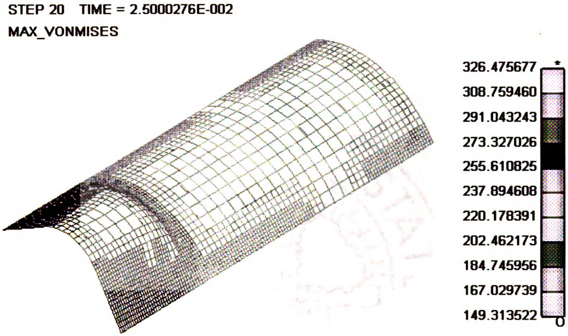

Figure (3.20) Von mises stress plot for the deformed tube before failure, after optimization.

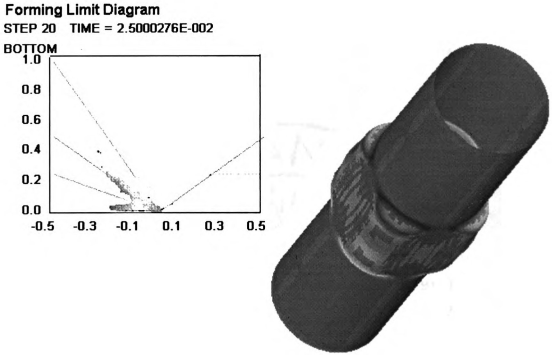

Figure (3.21) FLD plot for the deformed tube before failure, after optimization (full-scale model).

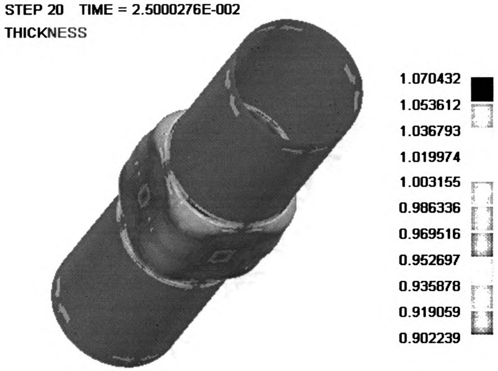

Figure (3.22) Thickness plot for the deformed tube before failure, after optimization (full-scale model).

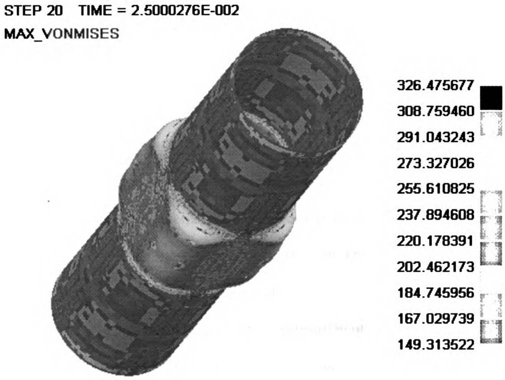

Figure (3.23) Von Mises stress plot for the deformed tube before failure after optimization (full-scale model).

CHAPTER 4

SUMMARY AND CONCLUSIONS

This thesis presents an approach to optimize the tube hydroforming process and consists of three major parts. A broad range of optimization topics was first reviewed which included past research involving a broad class in the optimization of engineering systems. The second section presented the tube hydroforming process and related theories in detail. The third section contained the simulation and optimization of tube hydroforming process. In the same section results before and after using HEEDS were discussed and experimental validation was presented.

Hydroforming is an emerging technology that meshes well with the automotive industry's drive to make more efficient material use. The application of this concept to structural parts leads to tubular box sections replacing stamped assemblies. Successful tube hydroforming process requires proper combination of part design, material selection, and application of internal pressure and axial feeding. By using finite element analysis methods, process parameters can be determined by manual optimization before manufacturing the dies and process development. The use of automated design optimization software to optimize the process parameters in a hydroformed part has never been attempted to date. This is the goal of the present work.

By using the optimal value of process parameters the tube expansion within the square die without failure is about 64% more as compared to manual optimization. That much expansion without failure was not possible with manual optimization of process parameters for the tube made of Aluminum 6061 with T6 condition that has very low value of strain hardening exponent. Only 8-10% reduction in thickness was noticed as shown in thickness plot in Figure (3.22).

REFERENCES

LIST OF REFERENCES

1. Bernd Viehweger, Esslingen/Germany, " Hydroforming applications in industry: Qualified equipment ensures economic use", conference, Innovation in Hydrofroming Technology, 1996, Nashville, Tennessee.

2. Keith Brewster, Kevin Sutter, Mustafa Ahmetoglu, and Taylan Altan, "A Review of Current Processes and Technology", conference, Innovation in Hydrofroming Technology, 1996, Nashville, Tennessee.

3. Murray Mason P. Eng, "Tube Hydroforming: Advancements Using Sequenced Forming Pressures," conference, Innovation in Hydrofroming Technology, 1996, Nashville, Tennessee.

4. F. Dohmann, Ch. Hartl, "Tube hydroforming – research and practical application", Journal of Materials Processing Technology 71 (1997) 174-186.

5. F. Dohmann, P. Bieeling, Werkzeugparameter und Prozeβdaten beim aufweitenden Innenhochdruckumformen, Umformtechnik 26 (1) (1992) 23-31.

6. Olhoff, N., Taylor. J.E., 1983, "On Structural Optimization", Journal of applied Mechanics, Vol. 50, pp. 1139-1151.

7. Stadler, W., and Dauer, J., 1992, "Multicriteria Optimization in Engineering: A Tutorial and Survey", Structural Optimization: Status and Promise, Progress in Astronautics and Aeronautics, vol. 150, AIAA Inc., pp. 209-249.

8. A. Böhm, Numerische Simulation von Verfahren der Innenhochdruckumformung unter besonderer Berücksichtigung des Aufweitens im geschlossenen Gesenk. Dissertation, UniversitätGH Paderborn, 1993.

9. F. Klaas, Aufweitstauchen von Rohren durch Innenhochdruckumformen. Fortschrittsbericht VDI, Reihe 2: Fertigungstechnik Nr. 42, Düsseldorf, and VDI-Verlag, 1987.

10. W. J. Sauer et al., Free bulge forming of tubes under internal pressure and axial compression, in: 6th North American Metal working Research Conference Proceedings, SME, Conference University of Florida, Gainsville 16-19 April 1978, pp. 228-235.

11. F. Dohmann, Ch. Hartl, Liquid-bulge-forming as a flexible production method, J. Mater. Process. Technol. 45 (1994) 37700382.

12. F. Klass, U. Lücke, and K. Kaehler, "Development of the Internal High-Pressure Forming Process," SAE, International Congress and Exposition, Detroit, Michigan, 1993.

13. H. Amino, K. Nakamura, and T. Nakagawa, "Counter-Pressure Deep drawing and Its Application in the Forming of Automobile Parts," Journal of Materials Processing Technology, volume 23 (1990), pp. 243-265.

14. Ingvar Rask and Dag Thuvesen, "Simulation of an engineering process – tube hydroforming" IVF – The Swedish Institute of Production Engineering Research.

15. Hosford, W. F. and Caddell, R. M., Metal Forming – Mechanics and Metallurgy, 1983, Prentice-Hall, Inc.

16. Brännberg N., "Computational Aspect on Simulation of Sheet Metal forming", Department of Mechanical engineering, Linökping Institute of Technology, Sweden, 1994.

17. Hallquist J.O., LS-DYNA Theoretical Manual, Livermore Software technology Corporation, Livermore, 1998.

18. Robert G. Whirley and Bruce E. Engelmann and Robert W. Logan, "Some Aspects of Sheet Forming Simulation using Explicit Finite Element Techniques", CED-Vol. 5/AMD Vol. 156, Numerical Methods for Simulation of Industrial Metal Forming Processes ASME 1992.

19. HEEDS Getting Started Manual by Applied Computational Design Associates, Inc. MI, 48864, USA.

20. General motors material testing laboratory, Raj k Mishra, raj.k.mishra@gm.com

21. I-DEAS Master Series, Theoretical Manual, Structural Dynamics Research Corporation, Milford, Ohio 45150.

22. Dynaform-PC, Theoretical Manual, Engineering Technology Associates, Inc. Troy, MI 48043.

23. VARI-FORM, "The ABSs of Hydroforming", Technical Journal, Chesterfield, MI 48051.

24. F. –U. Leitloff and W. Schäfer, "Hydroforming Applications in the Automotive Industry", conference, innovations in Hydroforming Technology, Tennessee, 1996.

25. ITC Interlaken Technology Corporation, "Hydroforming Press Brochure", Eden Prairie, MN 55344 USA.